Materials Research Express

Thermally induced phase transformations of Al₉₃Fe₄Nb₃ and Al₉₀Fe₇Nb₃ quenched alloys

To cite this article before publication: Olena Shved *et al* 2020 *Mater. Res. Express* in press https://doi.org/10.1088/2053-1591/ab79d1

IOP Publishing Journal Title
Journal **XX** (XXXX) XXXXXX https://doi.org/XXXX/XXXX

Thermally induced phase transformations of $Al_{93}Fe_4Nb_3$ and $Al_{90}Fe_7Nb_3$ quenched alloys

O.V. Shved[1], S.I. Mudry[1], V.O. Kotsyubynsky[2] and V.M. Boychuk[2]

[1] Physics of Metals Department, I. Franko Lviv National University, Lviv 79005, Ukraine
[2] Department of Material Science and New Technology, Vasyl Stefanyk Precarpathian National University, Ivano-Frankivsk 76018, Ukraine

E-mail: olenkawved01@gmail.com

Received xxxxxx
Accepted for publication xxxxxx
Published xxxxxx

Abstract

Al–based rapidly quenched alloys of composition $Al_{90}Fe_7Nb_3$ and $Al_{93}Fe_4Nb_3$ were studied by Mössbauer spectroscopy, X–ray powder diffraction and differential scanning calorimetry methods. The occurrence of thermally induced phase transformations has been established. It is shown that both ribbons reveal the structure in which Fe–atoms have an aluminum ones neighbors both in amorphous and annealed up to 653 K that corresponds to the atomic arrangement in Al_6Fe metastable phase. At higher than 709.6 K annealing temperatures the structural transformations of this phase into mix of stable $Al_{13}Fe_4$ compound and aluminium were observed and at 893 K these transformations were completed.

Keywords: Al–based alloys, quenching, crystallization

1. Introduction

Amorphous and nanocrystalline Al–Fe alloys (≥ 90 at. % Al) are promising structural and functional materials due to excellent properties combination – low density, high melting point, good wear resistance, high temperature strength and high resistance to creep and oxidation [1-3]. In particular, Al–Fe alloys had expanded their application as functional materials for electrochemistry and magnetoactive systems [4]. The development of ternary systems Al–Fe–TM(RE), where TM – transition and RE is rare earth metals, allows the obtaining of nanostructure alloys with improved properties, for instance, with high strength. In this case Al nanoclusters are embedded in an amorphous matrix, making in such way the nanocomposite system [5]. The detail investigations of thermally induced transformations in such systems allow to determine the effect of composition on the resulting strength and the ductile-brittle properties. Another important way is the possibility of quasicrystalline phase formation for Al–Fe–TM(RE) systems that have a fundamental scientific interest [6-8]. The alloy's properties notably depend on the synthesis methods (plasma spraying, ion irradiation, laser treatment, melt-spinning). The using of controllable rapid quenching allows obtaining the alloys with complex amorphous-nanocrystalline structure with the possibility of metastable phases (supersaturated solid solution and quasicrystals) formation [9]. In particular, during a quenching of binary Al–Fe alloys the formation of few metastable Al–based phases structurally related to icosahedral symmetry was observed [10]. Among Al–Fe–TM systems the Al–Fe–Nb alloys have an improved thermal stability with the possibility of Al cluster's size decreasing that in result allows to control alloys specific strength taking into account the different technological applications. The nanostructured Al–Fe–Nb alloys prepared by melt-spinning combine low Young's modulus, high microhardness and high corrosion resistance (both oxidation and sulphidation) [11-12]. The presence of Nb atoms allows obtaining the nanoquasicrystalline Al alloy with high strength, ductility and toughness combined with improved stability. Based on the preliminary data [12] quenched alloys of Al–Fe–Nb system reveal a glass-forming

ability ranging from 87 to 90 at. % of Al. At lower Al content alloys were found to be partially crystalline, but unfortunately at above content they were non-investigated. Therefore we have an interest in research near the upper limit of glass formation region.

On the other hand, at crystallization process causes the Al nanoclusters with different structure and as result with improved mechanical properties, first of all of better strength, can be formed [13]. So the detailed investigations of temperature induced changes of Al–Fe–Nb alloys nanostructure are important for obtaining functional materials with controllable characteristics.

2. Experimental

The ternary alloys $Al_{90}Fe_7Nb_3$ and $Al_{93}Fe_4Nb_3$ in the form of ribbons were prepared using melt-spinning method at cooling rate about 10^6 K/s as ribbons of about 30μm thickness. The vacuum annealing of obtained alloys was realized in temperature range from 653 to 893 K for 1 hour.

X-ray diffraction (XRD) data were collected using two types of diffractometers – STOE STADI P diffractometer [14] and DRON-3M devices equipped with a UVD-2000 high-temperature vacuum chamber. In both experiments Cu $K\alpha_1$-radiation, monochromatized with help of curved Ge (111) single crystal installed in primary beam were used. The temperature of the specimens was measured with a thermocouple of the chromel–alumel type. The full Rietveld analysis XRD obtained patterns was performed using FullProf.2k (version 5.40) software [15].

The Mössbauer spectra were measured using MS-1104Em spectrometer (^{57}Co(Cr) source, activity of about 45 mKi). The isomer shifts calibration was done respectively to α-Fe standard (line width 0.29 mm/s). The spectra analysis and fitting procedure were performed using UnivemMs 701 software.

Differential Scanning Calorimetry (DSC) test was performed using Pt–Rh crucible in the range from room temperature to 1073 K in helium atmosphere. Heating velocity was 20 K/min.

3. Results

XRD patterns of $Al_{93}Fe_4Nb_3$ and $Al_{90}Fe_7Nb_3$ samples obtained in a temperature range of 293-438 K (fig. 1,a,b) show the typical for amorphous alloys profile. It allow to assume that glass-forming range are wider than reported in [12] and as quenched alloys are amorphous up to 93 at. % of Al. The observed pre-peaks presence at about 25° is an evidence of intermediate order or quasicrystals formation process.

As follows from published data, the formation of close-ordered Fe- and Nb- centered nanoclusters is possible in this case. This type of structural ordering has been early observed for Al–Fe–Nb alloys in [16] and is characterized by high stability of Al–Fe bonds [17]. The main peak intensity is proportional to the differences scattering factors of the alloy constituent elements when its position corresponds to average interatomic distance R according to Ehrenfest formula [18]:

$$1.23\lambda = 2R\sin\theta \qquad (1)$$

Here λ is wavelength and θ – Bragg angle.

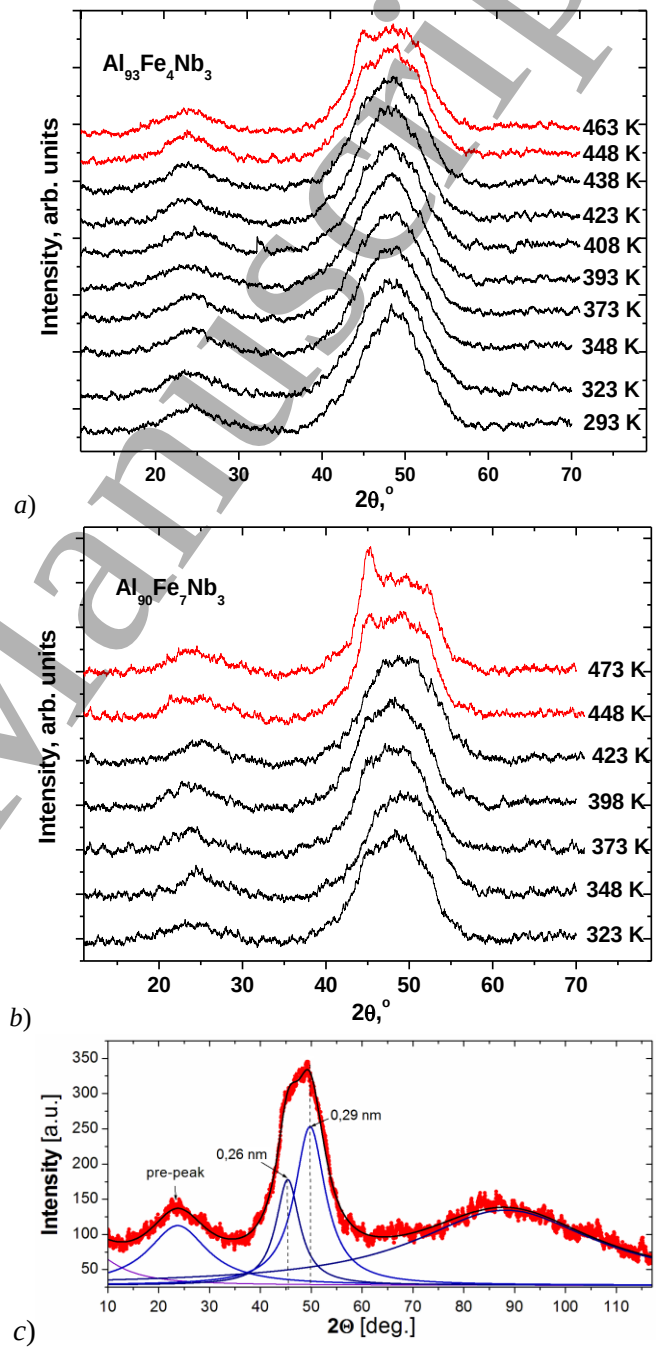

Fig.1. The XRD patterns of $Al_{93}Fe_4Nb_3$ (*a*,*c*) and $Al_{90}Fe_7Nb_3$ (*b*) alloys in a temperature range of 293-473 K (DRON-3M)

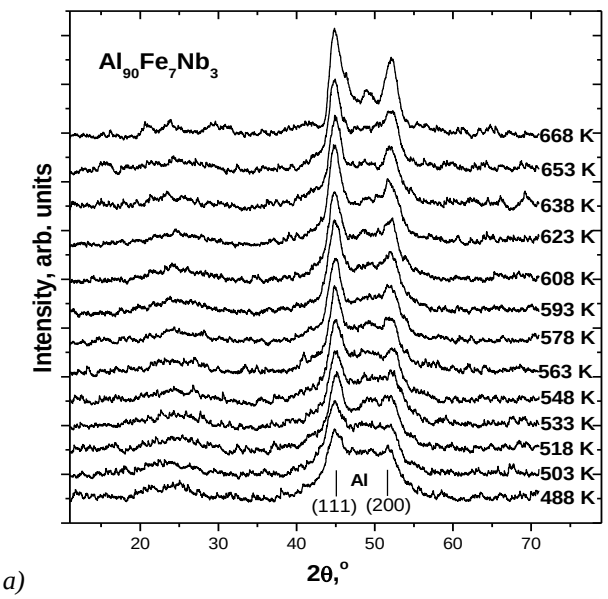

a)

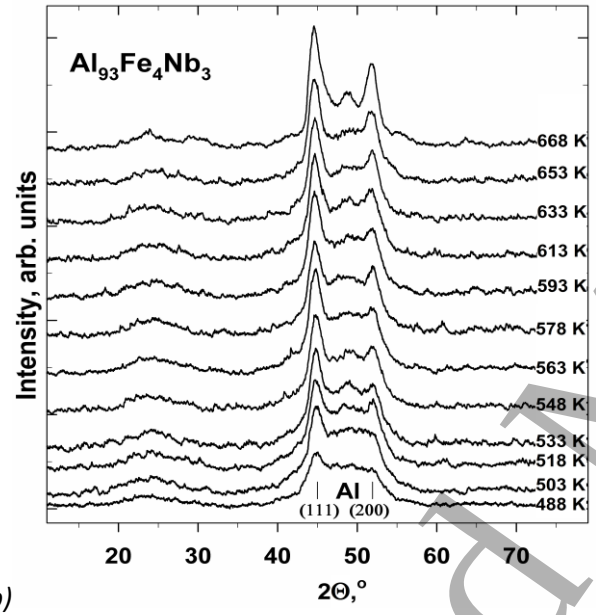

b)

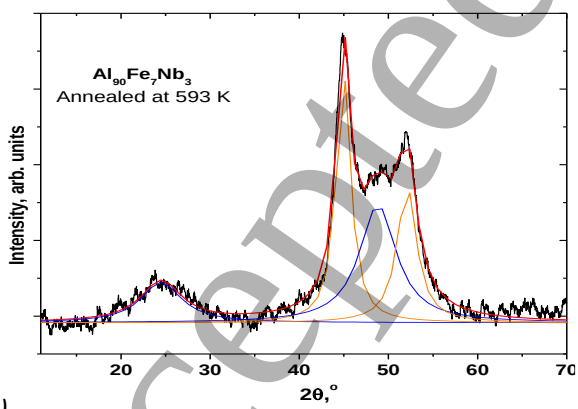

c)

Fig.2. The XRD pattern of (a) $Al_{90}Fe_7Nb_3$ alloy and (b) $Al_{93}Fe_4Nb_3$ in a temperature range of 488-668 K and (c) the Al phase reflexes separation for $Al_{90}Fe_7Nb_3$ alloy annealed at 593 K (DRON-3M)

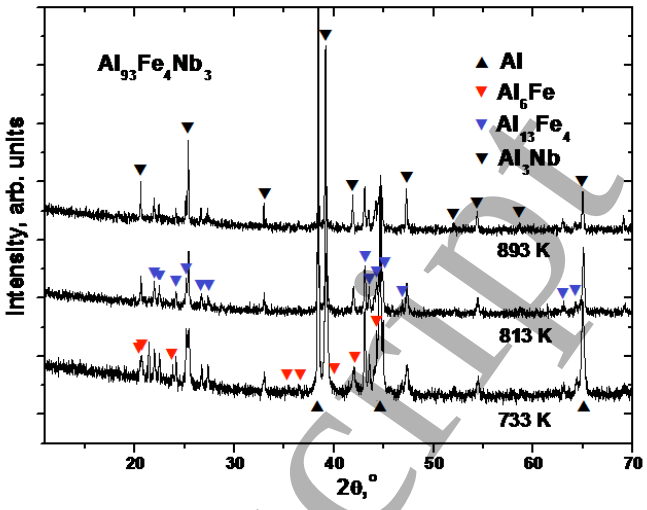

Fig.3. The XRD patterns of $Al_{93}Fe_4Nb_3$ alloy annealed at 733, 813 and 893 K (STOE STADI P)

The calculated interatomic distances corresponding to first subpeak of main peak (Fig. 1,*c*) at $2\theta \approx 50^o$ are about 0.25-0.28 nm that is close to Al–Fe distance for Al_6Fe phase [19], distance related to the second subpeak is 0,29 nm, which corresponds to Al. As is shown in [20] the position of the pre-peak is close to characteristics of icosahedral phases in the Al–Fe–V system. The second most probable interatomic distance calculated by (1) from pre-peak is about 0.52 nm that is close to the distance between transition metal atoms. The temperature increasing up to 448 K causes the beginning of Al phase crystallization with the appearance of (111) and (200) reflexes of Al phase in the main peaks (Fig. 2,a,b). The temperature of aluminum crystallization doesn't depend on the alloy's content. The separation of Al reflexes was performed using fitting with Lorentzian function (Fig. 2,c). The structural changes of alloys are similar. But in the case of $Al_{93}Fe_4Nb_3$ alloy nanocrystalline Al grains increase more rapidly, than in $Al_{90}Fe_7Nb_3$ alloy, which can be seen from the Al-reflexes of higher intensities and temperatures (Fig.2,b).

The volume fraction of nanocrystalline aluminum increases nonlinearly on annealing temperature. The average sizes of Al crystallites, calculated with using of Sherer's equation increase from 4 to about 14-16 nm at about 638 K for $Al_{90}Fe_7Nb_3$ and 18-20 nm for $Al_{90}Fe_7Nb_3$ alloys, respectively. Generally, the fast quenching of Al–Fe melt, in which Fe content range is of 2-12 at.%, can lead to formation of different types of metastable phases – orthorhombic Al_6Fe and Al_5Fe_2, tetragonal Al_mFe and monoclinic Al_9Fe_2 with close to icosahedral symmetry [21]. The formation of Al_6Fe metastable phase and $Al_{13}Fe_4$ compounds is possible for alloy, in which Fe content range is 2.3-9.2 at. %, whereas the formation of less stable crystal occurs at higher cooling rates. Three subpeaks corresponding to the interatomic distances in crystalline aluminum and Al_6Fe metastable phase have been

obtained by fitting procedure of main peak. In this phase Fe atoms are surrounded with 10 atoms of Al and interatomic distances are within a range of 0.24-0.26 nm (Fig. 3) [22]. The temperature increasing to about 650 K leads to more degree of structure ordering with the increasing of Al_6Fe phase content and the appearance of Al_3Nb cubic phase, in which Al atoms are partially substituted with Fe. The annealing at 733 K leads to changes of alloy phase composition with the domination of nanocrystalline aluminum and the presence of monoclinic $Al_{13}Fe_4$ phase. The observed changes correspond to Al_6Fe metastable phase decomposition in such way: $4Al_6Fe \rightarrow 11Al + Al_{13}Fe_4$. As it is shown by DSC test (Fig.4) this transformation takes place at 709.6 K. Further temperature increasing up to 893 K does not change the alloy phase composition.

Experimental Mössbauer spectra measured at room temperature for the as-prepared amorphous sample were fitted with two broadened quadrupole doublet components D1 (major) and D2 (minor) (Fig.5,a). These components have close isomeric shifts (IS_1=0.43 mm/s, IS_2=0.45 mm/s) and different values of quadrupole splitting (Δ_1=0.33 mm/s, Δ_2=0.57 mm/s) that can be explained by two different neighborhoods of Fe atoms. The size and electronegativity of Nb atoms is close to ones of Al, so the replacements process is possible.

It was observed early, that Al–Fe–Nb alloys, obtained by melt-spinning method, reveal the quascrystalline ordering, in which icosahedral Al–Fe–Nb-containing nanoparticles are embedded in Al matrix [24]. The stabiliting of icosahedral structure at the presence of TM was predicted with using the geometrical model [25].

The energy of icosahedral clusters increase with its growth due to space frustration effect and mismatching increasing between fcc- and ico-ordered clusters. The decreasing of space frustration is possible at substitution of Al atoms with Nb ones at icosahedral like atomic arrengement around the central Fe atom. It can be supposed that two doublet components of amorphous sample spectra correspond to two most probable types of Fe atoms icosahedral like atomic arrengement with the forming of Fe-centered icosahedral clusters.

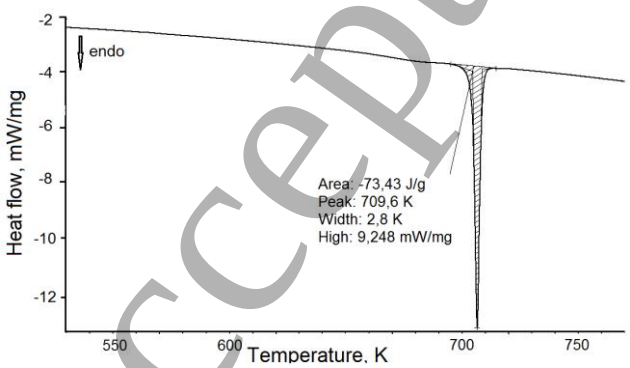

Fig. 4. DSC curve of heating process of $Al_{93}Fe_4Nb_3$ alloy

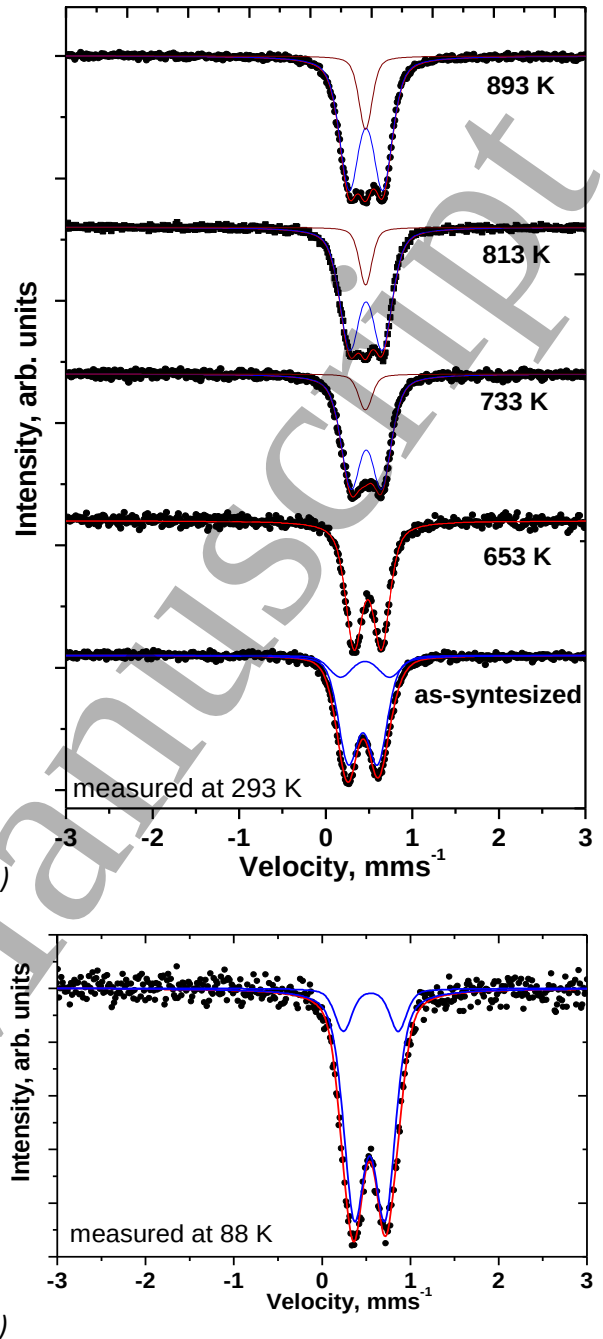

Fig.5. Mössbauer spectra of $Al_{93}Fe_4Nb_3$ alloy: (a) after annealing at 653, 733, 813, 893 K and measured at 293 K, (b) without annealing and measured at 88 K

At the same time the increasing of component's quadrupole splitting (new values are 0.35 and 0.65 mm/s, respectively) can be interpreted as a result of next space frustration optimization dominated only for less possible type of Fe atom short range order.

Lamb-Mössbauer factors for this sample measured using area method were found to be about 5.8±0.1 and 4.8±0.1% for spectra obtained at 293 and 88 K.

The Mössbauer spectra of as-synthesized $Al_{90}Fe_7Nb_3$ alloy also was fitted by two components with very close parameters (Fig.6,a). The major and minor doublet components intensity ratio is about 5:1 don't depends on temperature of spectra measurement. Lamb-Mössbauer factors for initial $Al_{90}Fe_7Nb_3$ sample are 4.9±0.1 and 5.0±0.2% at 293 and 88 K, respectively.

Mössbauer spectrum of $Al_{93}Fe_4Nb_3$ alloy annealed at 653 K show the structural changes and it is formed by single double component with IS=0.46 mm/s and Δ=0.32 mm/s. Accordingly to XRD data this component corresponded to Al_6Fe phase, in which Fe atoms have a unique close atomic order with ten nearest neighbors [25]. The unique type of Fe atoms close order corresponding to Al_6Fe phase was observed for $Al_{90}Fe_7Nb_3$ alloy annealed at 653 K too (Fig.6,a).

The increasing of annealing temperature causes the decomposition of Al_6Fe metastable phase and $Al_{13}Fe_4$ phase formation. The presence of $Al_{13}Fe_4$ phase is observed in room-temperature mössbauer spectra of alloys annealed at 733, 813 and 893 K. Similar phase transformation at thermal treatment of $Al_{90}Fe_7Nb_3$ alloy was observed in [6,7] and authors have interpreted spectrum with some contradiction for $Al_{13}Fe_4$ phase. The results of [7] were based on previous work [26], in which phase was fitted by three Lorentzians with equal width, but there was no explanation the spectrum components in terms of the structure. Crystal structure of $Al_{13}Fe_4$ is formed by Al–Fe stacked layers with five types of iron sites and two types of local arrangement, each of which has not spherical symmetry [27]. Therefore the spectrum should contain doublets only, one of which reveals very slight quadrupole splitting and looks like as singlet that is shown in [6,25,27].

The spectrum measured for $Al_{93}Fe_4Nb_3$ alloy annealed at 733 K was fitted by two doublet components D1 (IS=0.47 mm/s, Δ = 0.35 mm/s) and D2 (IS =0.46 mm/s, Δ = 0.05 mm/s). This result corresponds to layered structure of $Al_{13}Fe_4$ compound, in which four from five atomic sites with similar environment have formed one layer. So each doublet component can be assigned to the two types of iron sites, and D1 is a superposition of four atomic sites. The tendency to isomeric shift decrease and quadrupole splitting increase for D1 component with the annealing temperature increasing were observed (Fig. 7). It can be supposed similar to suppositions in other works [7] that quadrupole splitting increasing is the evidence of a grain growth. At the same time the quadropole splitting of D2 doubled component approaches to zero value. The observed processes are the result of thermally-induced structural re-arrangement with relaxation of microstresses and the increasing of Fe atoms relative content with spherical symmetry of short range order.

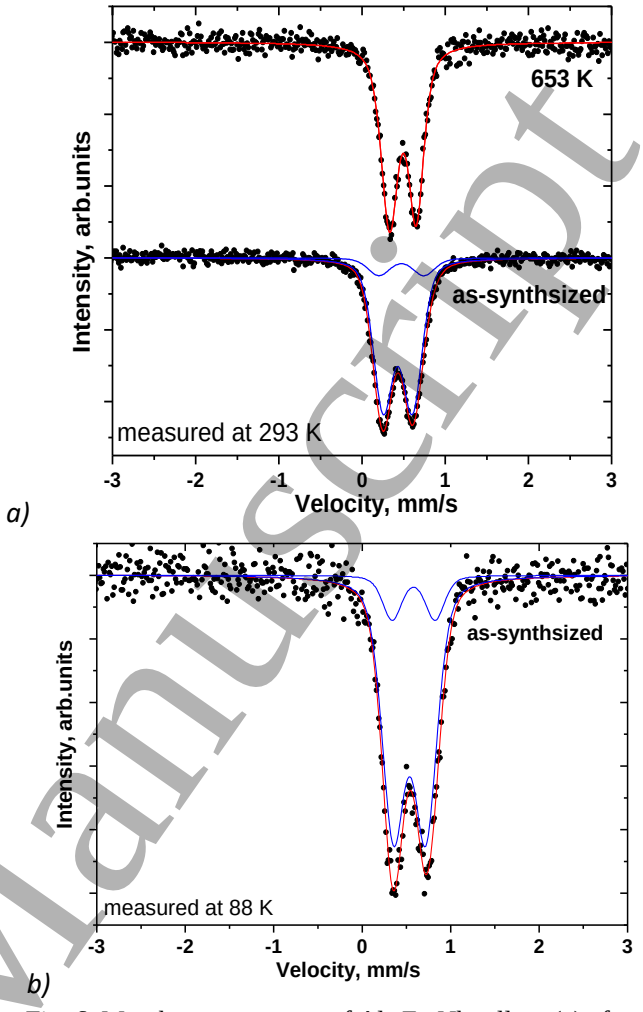

Fig. 6. Mössbauer spectrum of $Al_{90}Fe_7Nb_3$ alloy: (a) after annealing at 653 K and measured at 293 K, (b) without annealing and measured at 88 K

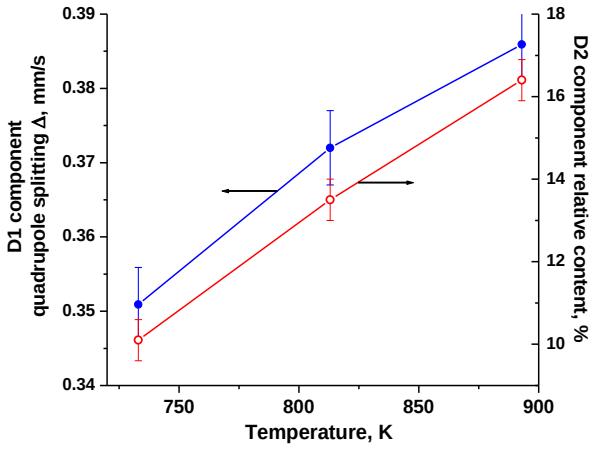

Fig.7. The temperature dependencies of D1 doublet component quadrupole splitting and D2 doublet component relative content for $Al_{93}Fe_4Nb_3$ alloys, annealed at 733, 813 and 893 K

The D1 to D2 integral inten sities ratio is about 5:1 and this is a probability of clusters formation with the different average numbers of Al and Nb in first coordination sphere of Fe atom. The mössbauer spectra measured for this sample at 88 K have a same composition (fig 6,a) and they were fitted by two doublet components D1 and D2. In fact the equal the temperature changes of isomeric shifts values were observed (IS_1=0.54 mm/s, IS_2=0.55 mm/s).

4. Conclusions

The thermally induced phase transformations of $Al_{90}Fe_7Nb_3$ and $Al_{93}Fe_4Nb_3$ rapidly quenched alloys have been investigated using XRD and Mössbauer spectroscopy methods in temperature range of 293-893 K. It was determined that up to 448 K both alloys show the formation of Fe-centered nanoclusters with icosahedral symmetry, embedded in amorphous Al matrix, which exist up to temperature of 709.6 K. Crystallization of Al is accompanied by metastable Al_6Fe phase nucleation and appearance of Al_3Nb cubic phase, in which Al atoms are partially substituted with Fe ones. The temperature increasing to 733 K causes the decomposition of Al_6Fe phase and $Al_{13}Fe_4$ compound formation. The further temperature increase leads to structural re-arrangement of $Al_{13}Fe_4$ related to microstresses relaxation and the increasing the Fe atoms number with spherical symmetry of short range order.

References

[1] Palm M 2009 Fe-Al materials for structural applications at high temperatures: current research at MPIE. *Int J Mater Res* **100** 277

[2] Audebert F, Idzikowski B, Švec P and Miglierini M 2005 Properties and Applications of Nanocrystalline Alloys from Amorphous Precursors. *NATO Sci Ser* **184** 301

[3] Inoue A 1998 Amorphous, nanoquasicrystalline and nanocrystalline alloys in Al-based systems, *Prog Mat Sci* **43** 365

[4] Sukiman N L, Zhou X, Birbilis N, Hughes A E, Mol J M C, Garcia S J & Thompson G E 2012 Durability and corrosion of aluminium and its alloys: overview, property space, techniques and developments *Aluminium Alloys-New Trends in Fabrication and Applications*, 47-97 DOI:10.5772/53752

[5] Inoue A, Kimura H 2001 Fabrications and mechanical properties of bulk amorphous, nanocrystalline, nanoquasi-crystalline alloys in aluminum-based system *J Light Met* **1** 31

[6] Parsamehr H, Lu Y J, Lin T Y, Tsai A P and Lai C H 2019 In-Situ observation of local atomic structure of Al–Cu–Fe quasicrystal formation *Sci Rep* **9** 1245

[7] Sitek J & Degmová J 2005 Aluminium based amorphous and nanocrystalline structure *Hyperfine Interact* **165** 121

[8] Sitek J & Degmová J 2006 Aluminium based amorphous and nanocrystalline alloys with Fe impurity *Czechoslovak Journal of Physics* **56** E17

[9] Shen Y, Perepezko J H 2017 Al-based amorphous alloys: Glass-forming ability, crystallization behavior and effects of minor alloying additions *J Alloys Compd* **707** 3

[10] Aliravci C A, Gruzleski J E, Pekgüleryüz M O 2013 A Thermodynamic study of Metastable Al-Fe Phase Formation in Direct Chill (DC)-Cast Aluminium Ingots *Essential Readings in Light Metals* **3** 466

[11] Audebert F, V´azquez S M, Guti´errez A, Vergara I, Alvarez G, Garc´ıa Escorial A, and Sirkin H 1998 Mechanical and Corrosion Behaviour of Al–Fe–Nb Amorphous Alloys *Mat Sci Forum* **269** 837

[12] Audebert F, Escorial A G and Sirkin H 1997 Aluminum-base Al–Fe–Nb amorphous and nanostructured alloys *Scripta Mat.* **36** 405

[13] Fan C, Yue X, Inoue A, Liu Ch-T, Shen X, Liaw P K 2019 Resent topics on the Structure and Crystallization of Al-based Glassy Alloys *Mat. Res.* **22** e20180619

[14] Stoe WinXPOW (version 3.03) 2010Stoe & Cie GmbH Darmstadt Germany

[15] Rodriguez-Carvajal J 1990 Fullprof: A Program for Rietveld Refinement and Pattern Matching Analysis, Abstract of the Satellite Meeting on Powder Diffraction of the XV Congress of the IUCr, Toulouse, France 127

[16] Audebert F, Arcondo B, Rodriguez D, Sirkin H 2001 Short Range Order Study in Al–Fe–X Melt Spun Alloys *Mat Sci Forum* **360-363** 155

[17] Illeková E, Janickovi D, Kubecka P, Švec P, Gachon J C 2004 Thermodynamic analysis of the clustering in the $Al_{90}Fe_7Nb_3$ alloy *Mat Sci Eng* A **375–377** 946

[18] Katz L 1964 X-ray diffraction in crystals, imperfect crystals, and amorphous bodies *Science* **142** 1564

[19] Villars P 2002 Pearson's Handbook Desk Edition, Crystallographic Data for Intermetallic Phases ASM International *Materials Park*

[20] Audebert F, Arcondo B, Rodriguez D, Sirkin H 2001 Short Range Order Study in Al–Fe–X Melt Spun Alloys *Mat Sci Forum* **360-362** 155

[21] Aliravci C A, Gruzleski J E, Pekgüleryüz M Ö 1998 A Thermodynamic Study of Metastable Al–Fe Phase Formation in Direct Chill (DC)-Cast Aluminum Alloy Ingots *Essential Readings in Light Metals* 466

[22] Holingsworth E H, Frank G R Jr 1962 Identification of a new Al–Fe constituent, $FeAl_6$ *Trans Metall Soc AIME* **224** 188

[23] Audebert F, Galano M & Saporiti F 2014 The use of Nb in rapid solidified Al alloys and composites *J Alloys Compd* **615** S621

[24] D. Herlach, D. Holland-Moritz, P. Galenko (Eds.), 2007 Metastable Solids from Undercooled Melts *Pergamon Materials Series* **10** Elsevier Germany

[25] Albedah M A, Nejadsattari F, Stadnik Z M & Przewoźnik J 2015 ^{57}Fe Mössbauer spectroscopy and magnetic study of $Al_{13}Fe_4$ *J Alloys Compd* **619** 839

[26] Forder S D, Brooks J S, Evans P V 1996 A Mössbauer investigation of phases formed in Al-Fe alloys *Scripta Mat.* **35** 1167

[27] Chittaranjan C M, Kumar V, Viswanathan B and Gopinathan K P 1991 Mössbauer study of $Al_{13}Fe_4$ *Solid state communications* **79** 69